Coherence, complexity and creativity[1]

FT Arecchi
Dept. of Physics, University of Firenze
Homepage:www.inoa,it/home/arecchi

Abstract

We review the ideas and experiments that established the onset of laser coherence beyond a suitable threshold. That threshold is the first of a chain of bifurcations in a non linear dynamics, leading eventually to deterministic chaos in lasers. In particular, the so called HC behaviour has striking analogies with the electrical activity of neurons. Based on these considerations, we develop a dynamical model of neuron synchronization leading to coherent global perceptions.
Synchronization implies a transitory control of neuron chaos. Depending on the time duration of this control, a cognitive agent has different amounts of awareness.
Combining this with a stream of external inputs , one can point at an optimal use of internal resources , that is called cognitive creativity.
While coherence is associated with long range correlations, complexity arises whenever an array of coupled dynamical systems displays multiple paths of coherence.
What is the relation among the three concepts in the title? While *coherence* is associated with long range correlations, *complexity* arises whenever an array of coupled dynamical systems displays multiple paths of coherence. *Creativity* corresponds to a free selection of a coherence path within a complex nest. As sketched above, it seems dynamically related to *chaos control*.

1 Introduction- Summary of the presentation

Up to 1960 in order to have a *coherent* source of light it was necessary to filter out a noisy regular lamp. Instead, the laser realizes the dream of shining a vacuum state of the electromagnetic field with a classical antenna, thus inducing a *coherent state* ,which is a translated version of the vacuum state ,with a minimum quantum uncertainty.
As a fact, the laser reaches its coherent state through a threshold transition ,starting from a regular incoherent source. Accurate photon statistics measurements proved the coherence quality of the laser as well the threshold transition phenomena ,both in stationary and transient situations .

The threshold is the first of a chain of dynamical bifurcations; in the 1980's the successive bifurcations leading to *deterministic chaos* were explored. Furthermore, the coexistence of many laser modes in a cavity with high Fresnel number gives rise to a *complex* situation, where the modes behave in a nested way, due to their mutual couplings, displaying a pattern of giant intensity peaks whose statistics is by no means Gaussian ,as in speckles.
Among the chaotic scenarios, the so called HC(*Heteroclinic chaos*), consisting of trains of equal spikes with erratic inter-spike separation, was explored in CO_2 and in diode lasers with feedback. It looks as the best implementation of a time code. Indeed, networks of coupled HC systems may reach a state of collective synchronization lasting for a finite time, in presence of a suitable external input. This opens powerful analogies with the *feature binding* phenomenon characterizing neuron organization in a perceptual task. The dynamics of a single neuron is suitably modelled by a HC laser; thence ,the collective dynamics of a network of coupled neurons can be realized in terms of arrays of coupled HC lasers [A.322] (for a guide to references see the note preceding the Bibliography) . Thus ,synchronization of an array of coupled chaotic lasers is a promising tool for a *physics of cognition.*

[1] Opening lecture at the 4-th Nat.Conf.on System Science,AIRS(Associazione Italiana Ricerca Sistemi), Trento 18 October 2007

Exploration of a *complex* situation would require a very large amount of time, in order to classify all possible *coherences* ,i.e. long range correlations. In cognitive tasks facing a *complex* scenario, our strategy consists in converging to a decision within a finite short time . Any conscious perception (we define conscious as that eliciting a decision) requires 200 msec, whereas the loss of information in the chaotic spike train of a single neuron takes a few msec.

The interaction of a *bottom-up* signal (external stimulus) with a *top-down* modification of the control parameters (induced by the semantic memory) leads to a collective synchronization lasting 200 msec: this is the indicator of a conscious perception. The operation is a *control of chaos,* and it has an optimality ; if it lasts less than 200msec, no decisions emerge, if it lasts much longer, there is no room for sequential cognitive tasks. We call *creativity* this optimal control of neuronal chaos. It amounts to select one among a large number of possible coherences all present in a complex situation. The selected coherence is the meaning of the object under study.

2. Coherence

2.1- Classical notion of coherence

Before the laser, in order to have a *coherent* source of light it was necessary to filter out a noisy regular lamp. **Fig1** illustrates the classical notion of coherence, with reference to the Young interferometer. A light source with aperture Δx illuminates a screen with two holes *A* and *B* (that we can move to positions *A'* and *B'*).We take the source as made of the superposition of independent plane waves, without mutual phase relations. The single plane wave is called *mode*, since it is a solution of the wave equation within the cavity containing the source. Each mode, passing through Δx , is diffraction broadened into a cone of aperture $\theta = \lambda / \Delta x$. At left of the screen, the light from *A* and *B* is collected on a detector, whose electrical current is proportional to the impinging light power, that is, to square modulus of the field. The field is the sum of the two fields E_1 and E_2 from the two holes. The modulus must be averaged over the observation time, usually much longer than the optical period; we call $< |E_1 + E_2|^2 >$ this average. The result is the sum of the two separate intensities $I_1 =< |E_1|^2 >$ and $I_2 =< |E_2|^2 >$, plus the cross phased terms $< E^*_1 E_2 > + < E^*_2 E_1 >$ .These last ones increase or reduce $I_1 + I_2$,depending on the relative phase, hence interference fringes are observed as we move the detector on a plane transverse to the light propagation, thus changing the path lengths of the two fields. Fringe production implies that the phase difference be maintained during the time of the average <…>, this occurs only if the two fields leaking through the two holes belong to the same mode, that is, if observation angle, given by the distance *AB* divided by the separation *r* between screen and detector, is smaller than the diffraction angle $\theta = \lambda / \Delta x$.

If instead it is larger, as it occurs e.g. when holes are in positions *A'* , *B',* then the detector receives contributions from distinct modes ,whose phases fluctuate over a time much shorter than the averaging time. Hence ,the phased terms are washed out and no fringes appear. We call *coherence area* that area S_{AB} on the screen which contains pairs of points *A,B* such that the collection angle be at most equal to the diffraction angle. S_{AB} subtends a solid angle given by

$$S_{AB} = \frac{\lambda^2 \cdot r^2}{(\Delta x)^2} \qquad (1)$$

The averaged product of two fields in positions *1=A* and *2=B* is called first order correlation function and denoted as

$$G^{(1)}(1,2) =< E_1^* E_2 > . \qquad (2)$$

In particular for *1=2*, $G^{(1)}(1,1) =< E_1^* E_1 >$ is the local intensity at point *1*. Points 1 and 2 correspond to holes *A* and *B* of the Young interferometer; their separation is space-like if the detector is at approximately the same distance from the holes. Of course, fringes imply path differences comparable with the wavelength, but anyway much shorter than the coherence time

$$\tau = 1/\Delta\omega \qquad (3)$$

of a narrowband (quasi-monochromatic) light source, indeed if the line breadth is much smaller than the optical frequency, $\Delta\omega << \omega$, then the coherence time is much longer than the optical period *T*, that is, $\tau >> T$.

In the case of the Michelson interferometer, 1and 2 are the two mirror positions, which are separated time-like. Fringe disappearance in this case means that the time separation between the two mirrors has become larger than the coherence time

2.2- Quantum notion of coherence

The laser realizes the dream of shining the current of a classical antenna into the vacuum state of an electromagnetic field mode, thus inducing a *coherent state* as a translated version of the vacuum state ,with a minimum quantum uncertainty.(**Fig. 2**)

We know from Maxwell equations that the a single field mode obeys a harmonic oscillator (HO) dynamics. The quantum HO has discrete energy states equally separated by $\hbar\omega$ starting from a ground (or vacuum) state with energy $\hbar\omega/2$ .Each energy state is denoted by the number *(0,1,2 ,..n,..)* of energy quanta $\hbar\omega$ above the ground state. In a coordinate *q* representation ,any state with a fixed *n* is delocalised, that is, its wavefunction is spread inside the region confined by the parabolic potential (see e.g. the dashed wave for *n=5*) .Calling *p=mv* the HO impulse , the *n* state has an uncertainty in the joint coordinate-impulse measurement increasing as

$$\Delta q \Delta p = (n + 1/2)\hbar . \qquad (4)$$

The vacuum state, with *n=0,* has the minimum uncertainty

$$\Delta q \Delta p = 1/2\hbar \qquad (4)'$$

If now we consider a version of the vacuum state translated by α (where α is proportional to *q*), this is a quantum state still with minimum uncertainty, but with an average photon number equal to the square modulus $|\alpha|^2$ (in the example reported in the figure we chose $|\alpha^2| = 5$). It is called *coherent state.* It oscillates at the optical frequency in the *q* interval allowed for by the confining potential. It maintains the instant localization ,at variance with a number state. The coherent state pays this coordinate localization by a Poisson spread of the photon number around its average $|\alpha|^2$.

The quantum field vacuum state shifted by a classical current had been introduced in 1938 by Bloch and Nordsieck; in 1963 R Glauber showed that these states have maximal coherence, and that a laser emits such a type of light, since the collective light emission in the laser process can be assimilated to the radiation of a classical current.

While the fringe production is just a test of the modal composition of the light field, the Hanbury Brown and Twiss interferometer (HBT) implies the statistical spread of the field amplitude.

HBT was introduced in 1956 as a tool for stellar observation (**Fig. 3**) in place of Michelson (M) stellar interferometer. M is based on summing on a detector the fields from two distant mirrors, in order to resolve the angular breadth of a star (that is, its diameter, or the different directions of two

stars in binary components). The more distant are the mirrors the higher the resolution. However the light beams deflected by the two mirrors undergo strong dephasing in the horizontal propagation and this destroys the fringes. In HBT, the two mirrors are replaced by two detectors, whose output currents feed a correlator; now the horizontal path is within a cable, hence not affected by further dephasing.
The working principle is intensity correlation (rather than field), which for a Gaussian statistics (as expected from thermal sources as the stars) yields the product of the two intensities plus the square modulus of the field correlation as provided by a standard interferometer, that is,

$$G^{(2)}(1,2) = < |E_1|^2 |E_2|^2 > = I_1 I_2 + |G^{(1)}|^2 \qquad (5)$$

Instead, Glauber had proved that for a coherent state, all the higher order correlation functions factor as products of the lowest one, that is,

$$G^{(n)}(1,2,...n) = G^{(1)}(1)G^{(1)}(2)...G^{(1)}(n) \qquad (6)$$

In particular, for n=2,we have

$$G^{(2)}(1,2) = G^{(1)}(1)G^{(1)}(2). \qquad (6)'$$

$G^{(1)}$ is just the intensity; thus a coherent state should yield only the first term of HBT, without the correlation between the two distant detectors.
In 1966 the comparison between a laser and a Gaussian field was measured time-wise rather than space-wise as shown in **Fig. 4.** The laser light displays no HBT, as one expects from a coherent state. The extra term in the Gaussian case doubles the zero time value. As we increase the time separation between the two *"instantaneous"* intensity measurements (by *instantaneous* we mean that the integration time is much shorter than the characteristic coherence time of the Gaussian fields),the extra HBT terms decays and eventually disappears. We have scaled the time axis so that HBT for different coherence times coincide. Coherence times are assigned through the velocities. of a random scatterer , as explained in the next sub-section.
Notice that fig. 4 reports coherence times of the order of 1msec.In the electronic HBT correlator, this means storing two short time intensity measurements (each lasting for example 50 nsec) and then comparing them electronically. If we tried to measure such a coherence time by a Michelson interferometer, we would need a mirror separation of the order of 300 km!

2.3-Photon statistics (PS)

As a fact, the laser reaches its coherent state through a threshold transition ,starting from a regular incoherent source. Accurate photon statistics measurements proved the coherence quality of the laser as well the threshold transition phenomena ,both in stationary and transient situations.
We have seen in fig.2 that a coherent state yields a Poisson spread in the photon number, that is, a photon number statistics as

$$p(n) = \frac{< n >^n}{n!} e^{-<n>} \qquad (7)$$

where $< n >= |\alpha|^2$ is the average photon number. This provides high order moments ,whereas HBT for eaual space-time positions 1=2 would yield just the first and the second moment .
Thus PS is statistically far more accurate, however it is confined to within a coherence area and a coherence time.
If now we couple the coherent state to an environment, we have a spread of coherent states given by a spread $P(\alpha)$.The corresponding PS is a weighted sum of Poisson distributions with different average values $< n >= |\alpha|^2$.
In **Fig.5** we report the statistical distributions of photocounts versus the count number. If the detector has high efficiency, they well approximate the photon statistics of the observed light source. We report measured oints (dots) as well as theoretical curves for three cases, namely, ***L***=laser light(coherent state); ***G***= Gaussian light; ***S***= superposition of the two fields ***L*** and ***G*** onto the same mode. The observation time *T* of each sample is much shorter than the coherence time of the Gaussian source; thus each measurement is "instantaneous".
A few words on how to build a Gaussian light source.A natural way would be to take a black-body source, since at thermal equilibrium $P(\alpha)$ is Gaussian. However its average photon number would be given by Planck's formula as

$$< n >= \frac{1}{\exp(-\hbar\omega / kT) - 1} \qquad (8)$$

For visible light $\hbar\omega = 2eV$ and current blackbody temperatures (remember that $10^4 K \approx 1eV$) we would have $< n ><< 1$. In order to produce much larger $< n >$,we shine a laser on a random scatterer .It consists of a grinded glass disc ,with scattering centers smaller than a wavelength and positioned at random distances from each other. As the disc rotates with a tangential velocity *v* at the site of the laser spots, it produces random speckles which lose coherence over a time inversely proportional to *v*. The coherence time may be of the order of 1 msec, as shown in fig.4, whereas the collection time of photons on the photocathode is of a few nanoseconds, thus practically *instantaneous.*

2.4- The laser threshold

Thus far L has been a laser well above threshold, satisfying Glauber's requirement the no reaction from the field be felt by the emitting atoms
We now explore how *PS* provides information on the threshold phenomena.
Let us simplify an atom as a two-level quantum system resonantly coupled to an optical field *E*. If the atom is in the ground state (**Fig.6**,upper part) it absorbs light and contributes a polarization *P* negative in the field $P = -\chi E$. The corresponding interaction energy $-P \bullet E$ is a convex parabola (upper right) and the corresponding equilibrium probability for the field has a maximum at the minimum of the parabola; in fact it is a Gaussian as expected for a blackbody field .
As the atom is excited to the upper state ,it will emit a photon and the polarization changes sign. The corresponding parabola is concave and the fields has no minimum where to be confined, but it should escape (left or right) toward high *E* values; no finite area probability could be defined. However ,as *E* achieves high values, a new fact occurs. The photon density in the cavity where the atom is contained increases , and there is a finite probability that the atom reabsorbs a photon going

again to the excited state and then re-emits a photon. The overall process, implying 3 photons, is less efficient than an independent photon emission from 3 excited atoms; thus it amounts to a negative correction of the polarization cubic in *E*. The corresponding energy is quartic in *E*; it has 2 minima symmetric around the origin. The field probability has 2 peaks at those minima. If the peaks are narrow, they can be assimilated to delta-like distributions at $+Eo$ and $-Eo$. The photon production is no sensitive to the phase difference ,thus we have a unique Poisson *PS* around $<n>=|Eo|^2$

As one increases the pump or reduces the cavity losses, a threshold is crossed where the stimulated emission gain compensates the losses. In **Fig.7** ,case 1 is below threshold with a confining parabola and a corresponding Gaussian field probability; case 3 is well above threshold with two narrow peaks of field probability . In between, case 2 (threshold: gain=losses) has zero linear polarization and hence a flat energy bottom ,yielding a broad probability distribution .

This means two things: i)a large value of the fluctuations around the average; ii) a slow dynamics within the flat potential well with corresponding long correlation times and narrow linewidth.

The laser threshold is like the critical point of a phase transition, displaying both i) critical fluctuations and ii)critical slowing down.

A formal approach is given in the Appendix .It summarizes the theory developed independently by the two groups of H.Haken and M.Lax, that the Landau classical theory of phase transitions in thermal equilibrium systems can be extended to non-equilibrium systems as the laser.

In **Fig.8** we report the behaviour of the second moment of PS, suitably scaled so that it is 1 for a Gaussian field and 0 for a coherent one, versus the ratio gain to losses expressed as ratio between M_1 (first order moment of *PS*, that is, laser intensity) and its threshold value M_{10}

The experimental points fit well Haken's theoretical line.

In **Fig.9** we plot the linewidth of the laser fluctuations versus the intensity ratio to threshold *I/Io*. The experiment fits the full solution λ_{eff} of the time dependent nonlinear Fokker Planck equation (see Appendix). A linear approximation yields a linewidth λ_{01} which is wrong around threshold.

2.5 - The transient laser

If we insert a fast shutter in a laser cavity where the atoms are highly pumped, as the shutter is switched from closed to open, the losses switch from a high value (above the gain) to a low value (below the gain).With reference to fig.7, the system has a sudden jump from case 1 to case 3. The transient in a He-Ne laser takes about 10 microsec. If we probe the *PS* over short observation times (50 nsec) at different delays from the switch time (Fig.10) we obtain different *PS* (normalized to equal area) ranging from the black-body statistics at the beginning (case a)to a Poisson statistics at the end (case f) . In order to collect the ensemble of experimental points of each *PS*, once a delay has been set and a single sample collected, the shutter is switched off and the measurement cycle repeated for that same delay.

If we extract first and second moments and plot average photon number $< n >$ and variance $< \Delta n^2 >=< n^2 > - < n >^2$ versus observation time,(Fig.11) we see that while the average has a monotonic increase the variance undergoes a large intermediate peak. The explanation is that the initial field fluctuations are initially linearly amplified, before being limited by the cubic gain saturation. Such a transient large fluctuation, observed in 1967 for a laser, was later observed in all second order phase transitions.

3.Deterministic chaos and complexity

3.1- Deterministic chaos

We know from Newton dynamics that, for assigned forces ,the trajectory emerging from a given initial condition ,as the star in **Fig.12,** is unique. The coordinates of the initial point are in general real numbers truncated to a finite number of digits, thus the initial condition is spread over a small patch. Points of the patch converge toward the calculated trajectory or diverge from it, depending on whether the transverse stability yields a stability landscape like a valley (left) or the ridge of a hill (right). Poincaré proved that from 3 coupled dynamical degrees of freedom on, the right situation is generic. Nowadays we call it *deterministic chaos* .It is a sensitive dependence on initial conditions and implies a loss of information of the initial preparation. The loss rate K is called Kolmogorov entropy. We can adjust its value by adding extra variables which change the slope of the downhill fall without practically perturbing the longitudinal trajectory (control of chaos)

In the case of the laser, the threshold is the first of a chain of dynamical bifurcations. Starting 1982, the successive bifurcations of a laser leading to *deterministic chaos* were explored. Among the chaotic scenarios, the so called HC(Heteroclinic chaos), consisting of trains of equal spikes with erratic interspike separation, was explored in CO_2 and in diode lasers with feedback **(Fig 13,14).** Fig.13 shows the experimental set up and displays the 3 coupled equations. The first two are the standard rate equations for the intensity x coupled to the population inversion y via the Einstein constant *G. ko* and γ are the damping rates for x and y, respectively, p_o is the pump rate. Two equations do not give chaos, and in fact a generic laboratory laser is not chaotic. We add a third equation as follows. The detected output intensity provides a voltage z which drives an intracavity loss modulator (see added z term in the first equations. In the feedback loop, R and b_o act as control parameters. The third damping rate β is of the same order as the other two.

The dynamics (Fig 14) consists of trains of almost equal intensity spikes, separated by erratic inter-spike intervals (ISI).In b) we zoom on two successive spikes, to show their repeatability. By a threshold we may cut the small chaotic fluctuations and observe a spiking of regular shape; however ,chaos results in the variable ISI.
In c) we build a 3-D phase space by an embedding technique. Each point reports the intensity sampled at time t and after two short delays τ and 2τ. The orbit closes at each turn (after a variable time depending on the local ISI). The figure is built over many spikes. The part of the orbit with a single line is the superposition of the large spikes, the small chaotic tangle corresponds to the small non-repetitive pulses.
The experimental phase space (fig.14c) suggests that is due to a saddle focus instability *S*, to which the system returns after a loop. The trajectory approaches *S* through a stable branch (**Fig.15**) ,or manifold, and escapes away through an unstable one. We call α the contraction rate and $\gamma \pm i\omega$ the complex expansion rate. If $\alpha < \gamma$ [Shilnikov] ,this local relation at *S* provides global chaos ,that we call *HC (homoclinic chaos*) since the return time to *S* is affected by the uncertainty in the expanding region, Around *S* the system displays a high susceptibility $\chi = response / stimulus$. Away from *S*, the system is insensitive to external perturbations and displays a repeatable loop. Time-wise, large spikes *P* of equal shape repeat at chaotic inter-spike intervals *(ISI).*
In fact the feedback laser has a second instability, a saddle node corresponding to zero intensity(see fig.14); in such a case *HC* stays rather for *heteroclinic chaos.*
Due to the high susceptibility, a small perturbation applied around *S* strongly affects the *ISI*; we exploit this fact to synchronize the HC laser to an external signal. If the driving frequency is close to the natural one (associated with the average <*ISI*>) we have a 1:1 locking.
Fig.16 shows the laser synchronization to a small forcing signal .In the feedback amplifier we introduce a periodic input which is a small percentage of the feedback signal. A forcing frequency close to $2\pi / < ISI >$ induces a 1.1 locking; at lower frequencies we have 1:2 and 1:3 locking, at higher frequencies we have 2.1 etc locking regimes.

It looks as the best implementation of a time code: indeed, networks of coupled HC systems may reach a state of collective synchronization lasting for a finite time, in presence of a suitable external input. This opens powerful analogies with the *feature binding* phenomenon characterizing neuron organization in a perceptual task(Sec.4)

3.2-Complexity of a multimode light oscillator

a)longitudinal case

Thus far we have referred to laser cavities designed to house one or a few transverse modes. In fact, if L is the mirror separation and d the mirror diameter, the number of diffraction angles λ / d that can be seen by the aperture angle d/L is given by the Fresnel number

$$F = \frac{d^2}{\lambda L}$$

For example in a gas laser $L=1m, \lambda \approx 10^{-6} m,$ and $d \approx 10^{-3} m$,so that $F \approx 1.$,
and the laser cavity hosts a single transverse mode.
If however the gain line is much larger than the longitudinal mode separation
$\Delta \nu_{gain} >> c/2L$,
then many longitudinal modes can be simultaneously above threshold. In such a case the nonlinear mode-mode coupling, due to the medium interaction, gives an overall high dimensional dynamical system which may undergo chaos. This explains the random spiking behaviour of long lasers. The regular spiking in time associated with mode locking is an example of mutual phase synchronization, .akin to the regular spiking reported in fig. 16.

b) transverse case

Inserting a photorefractive crystal in a cavity, the crystal is provided high optical gain by a pump laser beam. As the gain overcomes the cavity losses ,we have a coherent light oscillator Due to the narrow linewidth of the crystal, a single longitudinal mode is excited; however, by an optical adjustment we can have large Fresnel numbers ,and hence many transverse modes. We carried a research line starting 1990 [A.177,183,etc; review in 202]. Recently we returned to this oscillator but with a giant photorefractive effect provided by the coupling of a photorefractive slice to a liquid crystal [A.341,350,355].(**Fig.17**). The inset in this figure shows how phase singularities appear in a 2D wave field. A phase gradient circulation $\pm 2\pi$ is called a topological charge of ± 1 respectively. A photodetector responds to the modulus square of the field amplitude. To have a phase information, we superpose a plane wave light to the 2D pattern, obtaining results illustrated in **Fig.18**.For a high Fresnel number we have a number of singularities scaling as the square of the Fresnel number [A.197].Referring to the inset of Fig.17,when both intersections of the two zero lines are within the boundary, we expect a balance of opposite topological charges. However, for small Fresnel numbers ,it is likely that only one intersection is confined within the boundary; this corresponds to an unbalance ,as shown in Fig.18, upper right.
The scaling with the Fresnel number is purely geometric and does not imply dynamics.
The statistics of zero-field occurrences can be predicted on purely geometric considerations, as done for random speckles
If instead we look at the high intensity peak in between the zeros, the high fields in a nonlinear medium give a strong mode-mode coupling which goes beyond speckles.
This should result from the statistical occurrence of very large peaks. In order to do that ,we collect space-time frames as shown in **Fig.19**,with the help of the CCD +grabber set up shown in Fig.17. We don't have yet a definite 2D comparison with speckles. However , a 1D experiment in an optical fibre has produced giant optical spikes with non-Gaussian statistics [Solli et al.]The author draw an analogy with the so called "rogue" wave in the ocean which represent a frequent

problem to boats, since satellite inspection has shown that they are more frequent than expected on a purely linear basis.
We consider the anomalous statistics of giant spikes as a case of complexity, because the mutual coupling in a nonlinear medium makes the number of possible configurations increasing exponentially with the Fresnel number ,rather than polynomially.
The rest of the paper explores this question: how it occurs that a cognitive agent in a complex situation decides for a specific case, before having scanned all possible cases ,that is, how we "cheat" complexity.

4. Physics of cognition – Creativity

4.1-Perception and control of chaos

Synchronization of a chain of chaotic lasers provides a promising model for a *physics of cognition.* Exploration of a *complex* situation would require a very large amount of time. In cognitive tasks facing a *complex* scenario, our strategy consists in converging to a decision within a finite short time . Various experiments [Libet, Rodriguez et al.] prove that a decision is taken after 200 ms of exposure to a sensory stimulus Thus, any conscious perception (we define conscious as that eliciting a decision) requires about 200 msec, whereas the loss of information in a chaotic train of neural spikes takes a few msec.

Let us consider the visual system; the role of elementary feature detectors has been extensively studied [Hubel]. By now we know that some neurons are specialized in detecting exclusively vertical or horizontal bars, or a specific luminance contrast, etc. However the problem arises: how elementary detectors contribute to a holistic (*Gestalt*) perception? A hint is provided by [Singer]. Suppose we are exposed to a visual field containing two separate objects. Both objects are made of the same visual elements, horizontal and vertical contour bars, different degrees of luminance, etc. What are then the neural correlates of the identification of the two objects? We have one million fibers connecting the retina to the visual cortex. Each fiber results from the merging of approximately 100 retinal detectors (rods and cones) and as a result it has its own receptive field. Each receptive field isolates a specific detail of an object (e.g. a vertical bar). We thus split an image into a mosaic of adjacent receptive fields.
Now the "*feature binding*" hypothesis consists of assuming that all the cortical neurons whose receptive fields are pointing to a specific object synchronize the corresponding spikes, and as a consequence the visual cortex organizes into separate neuron groups oscillating on two distinct spike trains for the two objects.
Direct experimental evidence of this synchronization is obtained by insertion of microelectrodes in the cortical tissue of animals just sensing the single neuron (**Fig.20**)[Singer].
An array of weakly coupled HC systems represents the simplest model for a physical realization of feature binding. The array can achieve a collective synchronized state lasting for a finite time (corresponding to the physiological 200 ms!) if there is a sparse (non global) coupling, if the input (bottom-up) is applied to just a few neurons and if the inter-neuron coupling is suitably adjusted(top-down control of chaos) [A.322; Ciszak,Montina and Arecchi, to be published].
Fig.21 shows the scheme of ART [S.Grossberg]

The interaction of a *bottom-up* signal (external stimulus) with a *top-down* change of the control parameters (induced by the semantic memory) leads to a collective synchronization lasting 200 msec: this is the indicator of a conscious perception. The operation is a *control of chaos,* and it has an optimality ; if it lasts less than 200msec, no decisions emerge, on the contrary, if it lasts much longer, there is no room for sequential cognitive tasks(**Fig.22**)
The addition of extra degrees of freedom implies a change of code, thus it can be seen as a new level of description of the same physical system.

4.2- From perception to cognition - Creativity

We distinguish two types of cognitive task. In *type I*, we work within a prefixed framework and readjust the hypotheses at each new cognitive session, by a Bayes strategy. Bayes theorem [Bayes] consists of the relation:

$$P(h \mid data) = P(data \mid h)\, P(h)/P(data) \qquad (9)$$

That is: the probability $P(h \mid data)$ of an hypothesis *h*, conditioned by the observed *data* (this is the meaning of the bar |) and called *a-posteriori probability of h*, is the product of the probability $P(data \mid h)$ that *data* is generated by an hypothesis *h*, times the a-priori probability $P(h)$ of that hypothesis (we assume to have a package of convenient hypotheses with different probabilities) and divided the probabilty $P(data)$ of the effectively occurred data. As shown in Fig. 23, starting from an initial observation and formulating a large number of different hypotheses, the one supported by the experiment suggests the most appropriate dynamical explanation. Going a step forward and repeating the Bayes procedure amounts to climbing a probability mountain along a steepest gradient line.
On the other hand, a complex problem is characterized by a probability landscape with many peaks (Fig. 24). Jumping from a probability hill to another is not Bayesian; I call it *type II* cognition. A deterministic computer can not do it.

In human cognition, *type II* is driven by hints suggested by the context (*semiosis*) yet not included in the model. *Type II* task is a *creativity* act because it goes beyond it implies a change of code, at variance with *type I,* which operates within a fixed code. . The ascent to a single peak can be automatized in a steepest gradient program; once the peak has been reached, the program stops, any further step would be a downfall. A non-deterministic computer can not perform the jumps of *type II*, since it intrinsically lacks semiotic abilities. In order to do that, the computer must be assisted by a human operator. We call "meaning" the multi-peak landscape and "semantic complexity" the number of peaks. However, this is a fuzzy concept, which varies as our comprehension evolves.

Let us discuss in detail the difference between *type I cognitive task,* which implies changing hypothesis *h within a model,* that is, climbing a single mountain, and type *II cognitive task* which implies *changing model,* that is, jumping over to another mountain.

We formalize a model as a set of dynamical variables *xi (i=1,2,…N) ,N* being the number of degrees of freedom, with the equations of motion

$$\dot{x}_i = F_i(x_1 \ldots, x_N; \mu_1 \ldots, \mu_M) \qquad (10)$$

Where F_i are the force laws and the *M* numbers μ_i represent the *control parameters*; .The set **{F,x,** μ **}** is the model.

Changing hypotheses within a model means varying the control parameters, as we do when exploring the transition from regular to chaotic motion in some model dynamics.

Instead, *changing code, or model,* means selecting different sets $\boldsymbol{y}, \nu, \boldsymbol{G}$ of degrees of freedom, control parameters and equations of motion as follows:

$$\dot{y}_i = G_i(y_1 ..., y_R; \nu_1 ..., \nu_L) \qquad (11)$$

Where R and L are different respectively from N and M. The set $\{\mathbf{G},\mathbf{y},\nu\}$ is the new model.

While changing hypotheses within a model is an a-semiotic procedure that can be automatized in an computerized *expert system,* changing model implies catching the meaning of the observed world, and this requires what has been called *embodied cognition* [Varela]. Embodied cognition has been developed over thousands of generations of evolutionary adaptation, and we are unable so far to formalize it as an algorithm.

This no-go statement seems to be violated by a class of complex systems, which has been dealt with successfully by recursive algorithms. Let us consider a space lattice of spins, with couplings that can be ferro or anti-ferromagnetic in a disordered, but frozen way (spin glass at zero temperature, with quenched disorder). It will be impossible to find a unique ground state. For instance having three spins A, B, and C in a triangular lattice, if all have ferromagnetic interaction, then the ground state will consist of parallel spins, but if instead one (and only one) of the mutual coupling is anti-ferromagnetic, then there will be no satisfactory spin orientation compatible with the coupling (try with: A-up, B-up, C-up; it does not work; then try to reverse a single spin, but it does not work either).

This model has a cognitive flavor, since a brain region can be modeled as a lattice of coupled neurons with coupling either excitatory or inhibitory, thus resembling a spin glass, [Hopfield, Amit, Toulouse]. We have a large number of possible ground states, all including some frustration. Trying to classify all possible configurations is a task whose computational difficulty (either, program length or execution time) diverges exponentially with the size of the system. Sequentially related changes of code have been successfully introduced to arrive at finite-time solutions. [Mezard et al, Solomon].

Can we say that the mentioned solutions realize the reductionistic dream of finding a suitable computer program that not only climbs the single probability peak, but also is able to chose the highest peak? If so, the optimization problem would correspond to understanding the *meanin*g of the object under scrutiny.

We should realize however that spin glasses are frozen objects, given once for ever. A clever search of symmetries has produced a spin glass theory [Mezard et al] that, like the Renormalization Group (RG) for critical phenomena [Wilson] discovers a recursive procedure for changing codes in an optimized way. Even though the problem has a large number of potential minima, and hence of probability peaks, a suitable insight in the topology of the abstract space embedding the dynamical system has led to an optimized trajectory across the peaks. In other words, the correlated clusters can be ordered in a hierarchical way and a formalism analogous to RG applied.

It must be stressed that this has been possible because the system under scrutiny has a structure assigned once for ever. In everyday tasks, we face a system embedded in an environment, which induces a-priori unpredictable changes in course of time. This rules out the nice symmetries of hierarchical approaches, and rather requires an adaptive approach. Furthermore, a real life context sensitive system has to be understood within a reasonably short time, in order to take vital decisions about it.

We find again a role of control of chaos in cognitive strategies, whenever we go beyond the limit of a Bayes strategy. We call *creativity* this optimal control of neuronal chaos .
Four cases of creative science are listed in Table 1.
Furthermore, **Fig.24** sketches the reduction of complexity and chaos which results from a creative scientific step.

Table 1-From complication to complexity: four cases of creativity

1 - electricity - magnetism– optics	*Electromagnetic equations (Maxwell)*
2- Mendeleev table	*Quantum atom (Bohr, Pauli)*
3 - zoo of 200 elementary particles	*Quarks (M Gell Mann)*
4 – scaling laws in phase transitions	*Renormalization group (K.Wilson)*

Appendix [Haken, Lax]

Haken theory of laser threshold

We summarize in Table 2 the Langevin equation for a field E , ruled by a dynamics $f(E)$ corresponding to the atomic polarization and perturbed by a noise. The noise has zero average and a delta-like correlation function with amplitude D given by the spontaneous emission of the N_2 atoms in the upper state.

The time dependent probability *P(E,t)* for *E* obeys a Fokker-Planck equation. In the stationary limit of zero time derivative, the Fokker-Planck equation is easily solved and gives a negative exponential on *V(E)* which is the potential of the force *f(E)*.
Below laser threshold, *f(E)* is linear ,*V* quadratic and *P(E)* Gaussian. Above threshold, *f* has a cubic correction , *V* is quartic and *P(E)* displays two peaks at the minima of the quartic potential.

Table 2

$$\dot{E} = f(E) + \xi \quad \longleftarrow \textbf{Eq. di Langevin}$$

$$< \xi_0 \xi_t >= 2D\delta(t)$$

$$D = \gamma_{spont} N_2$$

$$\frac{\partial P}{\partial t} = -\frac{\partial}{\partial E} f(E) + D\frac{\partial^2 P}{\partial E^2} \quad \longleftarrow \textbf{Eq. di Fokker-Planck}$$

$$P(E) \approx e^{-V(E)/D} \quad \longleftarrow \textbf{soluzione stazionaria}$$

$$V(E) = -\int f(E)dE$$

$$f(E) = -\alpha E$$

$$f(E) = +\alpha E - \beta |E|^2 E \quad \longleftarrow \textbf{leggi forza ,sotto/sopra soglia}$$

References
References are listed in alphabetic order.
Since the topics of this review track my research line along the years , those papers of which I am author or co-author are referred to by A- followed by the number assigned to that paper in my homepage:
www.inoa.it/home/arecchi
List of publications - Research papers in Physics
(for instance, in the caption of Fig.25 , [A.25] means: FT Arecchi,E Gatti and a Sona, Phys. Lett., 20, 27 (1966).)

- DJ Amit, H Gutfreund ,and H Sompolinski , Phys. Rev A32, 1007 (1985)
- T. Bayes, Phil. Trans. Royal Soc. London 53, 370-418 (1763)
- GJ Chaitin "*Algorithmic information theory*", Cambridge University Press 1987
- M. Ciszak,A.Montina and FTArecchi,to be published (2008)
- RJ Glauber, Phys.Rev.130, 2529 (1963) ; 131,2766 (1963) ; in *Quantum Optics and*

Electronics ,edited by C. DeWitt et al, (Gordon and Breach ,New York,1965)

- S Grossberg, The American Scientist, 83,439 (1995)

- H. Haken, Phys.Rev.Lett.13,329(1964); H Haken, H Risken and W Weidlich Zeits.Phys.204,223(1967); 206, 355 (1967)

- JJ Hopfield, Proc.Nat.Aca.Sci.USA 79,2554(1982)

- D.H. Hubel, *Eye, Brain and Vision*, Scientific American Library, No. 22, W.H. Freeman, New York,1995.

- B. Libet, E.W. Wright, B. Feinstein, D.K. Pearl, *Subjective referral of the timing for a conscious sensory experience,* Brain 102 (1979) 193.

- M Mezard, G Parisi, MA Virasoro, *Spin glass theory and beyond,* World Scientific, Singapore,1987;

- E. Rodriguez, N. George, J.P Lachaux, J. Martinerie, B. Renault, F. Varela, Nature 397 340–343(1999)

- TA Sebeok,*Biosemiotics:its roots, proliferation,and prospects* Semiotica,1341/4,61-78 (2001);

- A. Shilnikov, L. Shilnikov and D. Turaev, Int. J. Bif. And Chaos 14, 2143 (2004).

- H.A. Simon (1980). *Cognitive science: The newest science of the artificial*. Cognitive Science, 4, 33-46.

- W. Singer and E. C. M. Gray, Annu. Rev. Neurosci. 18 555 (1995);

- DR Solly, C Ropers, P Koonath and B Jalali, Nature, 450, 1054 (2007)

-- S Solomon, *The microscopic representation of complex macroscopic phenomena,* Ann. Rev. of Comp. Physics II,pp:243-294 (World Scientific,1995).

- G Toulouse, S Dehaene, and JP Changeux, Proc. Nat. Aca. Sci. USA 83, 1695 (1986)

- F. Varela, E. Thompson, E. Rosch, *The Embodied Mind*, MIT Press, Cambridge, MA, 1991.

- K.G Wilson , Rev. Mod. Phys. **47**, 773 (1975)

Coherence, complexity and creativity
FT Arecchi

AIRS 07 Figs+ captions

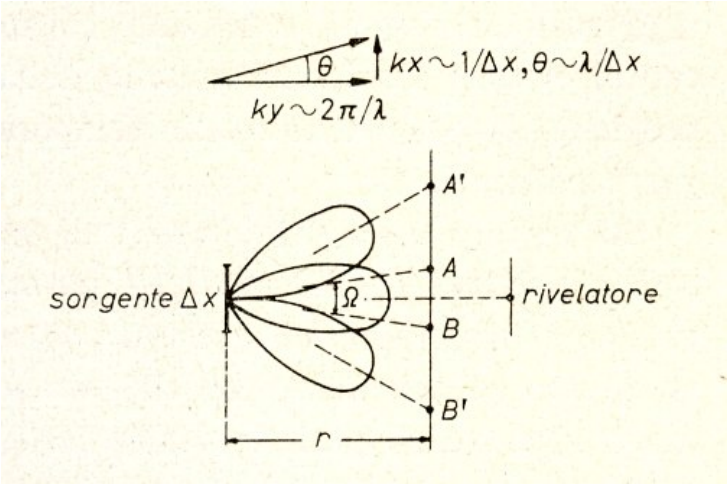

Fig.1- Young interferometer : a light source of aperture Δx illuminates a screen with two holes in it. Under suitable conditions, the phase interference between the fields leaking trough the two holes gives rise to interference fringes, as the point like detector is moved on a plane transverse to the propagation direction.

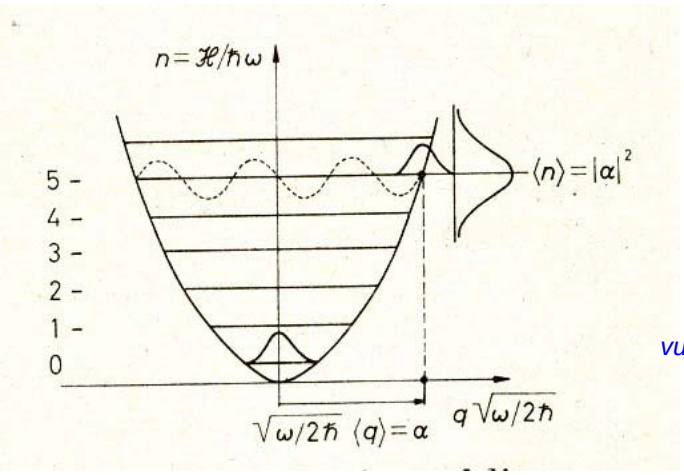

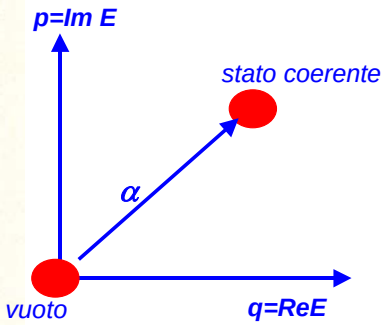

$$\Delta q \Delta p = (n + 1/2)\hbar \qquad \Delta q \Delta p = 1/2\hbar$$

$$G^{(n)}(1,2,...n) = G^{(1)}(1)G^{(1)}(2)...G^{(1)}(n)$$

Fig.2-Quantum harmonic oscillator in energy-coordinate diagram . Discrete levels correspond to photon number states . A coherent state is a translated version of the ground state; its photon number is not sharply defined but is spread with a Poisson distribution.

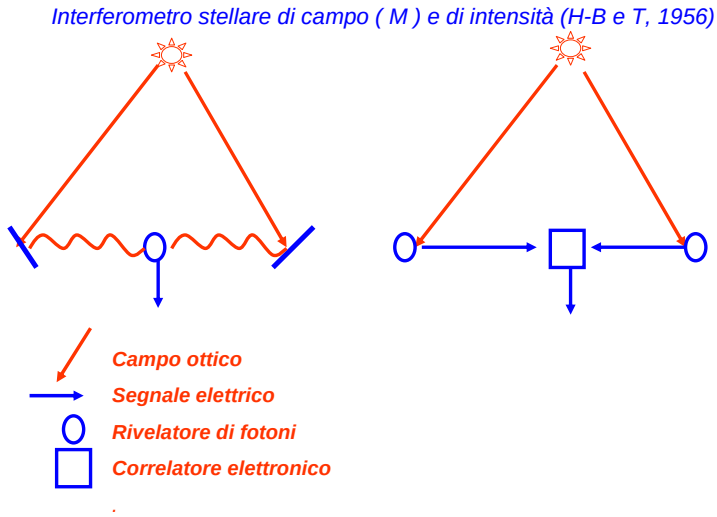

Fig.3 Left: the Michelson stellar interferometer M ;it consists of two mirrors which collect different angular views of a stellar object and reflect the light to a single photon detector through long horizontal paths (10 to 100 meters) where the light phase is affected by the ground variations of the refractive index (wavy trajectories).

Right: the Hanbury-Brown and Twiss (HBT) interferometer; mirrors are replaced by detectors and the current signal travel in cables toward an electronic correlator, which performs the product of the two instant field intensities $E_1^* E_1, E_2^* E_2$ and averages it over a long time.

Hanbury-Brown e Twiss: correlazione di intensità

$$G^{(2)}(1,2) = \langle |E_1|^2 |E_2|^2 \rangle = I_1 I_2 + |G^{(1)}|^2$$

proprietà processi gaussiani

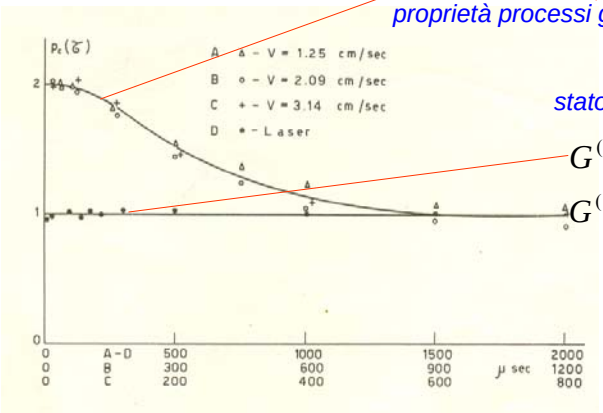

stato coerente

$$G^{(2)} = \left[G^{(1)}\right]^2,$$

$$G^{(n)} = \left[G^{(1)}\right]^n,$$

(Arecchi,Gatti,Sona-1966)

Fig4-Laboratory measurement of HBT for Gaussian light sources with different coherence times; for each case, the first order correlations between the signals sampled at different times decay with the respective coherence time, and asymptotically only the product of the average intensities (scaled to 1) remains. The laser light displays no HBT, as one expects from a coherent state.[A.25]

Distribuzioni statistiche dei fotoconteggi (Arecchi, 1965)

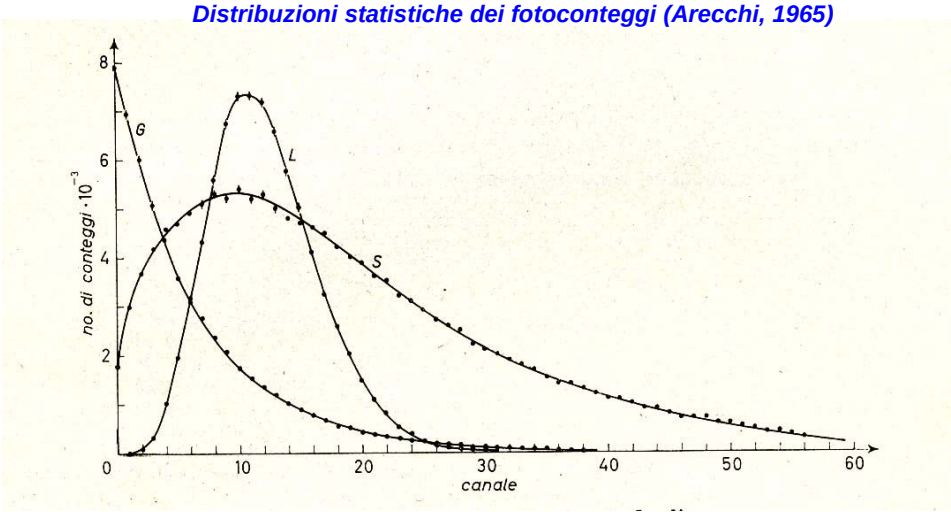

L=luce laser; G= luce gaussiana; S= sovrapposizione dei due campi

Fig.5-Statistical distributions of photocounts versus the count number. If the detector has high efficiency, they well approximate the *PS* of the observed light. ***L***=laser light; ***G***= Gaussian light; ***S***= superposition of the two fields ***L*** and ***G*** onto the same mode. The observation time *T* of each sample is much shorter than the coherence time of the Gaussian source; thus each measurement is *"instantaneous*".[A.23,30]

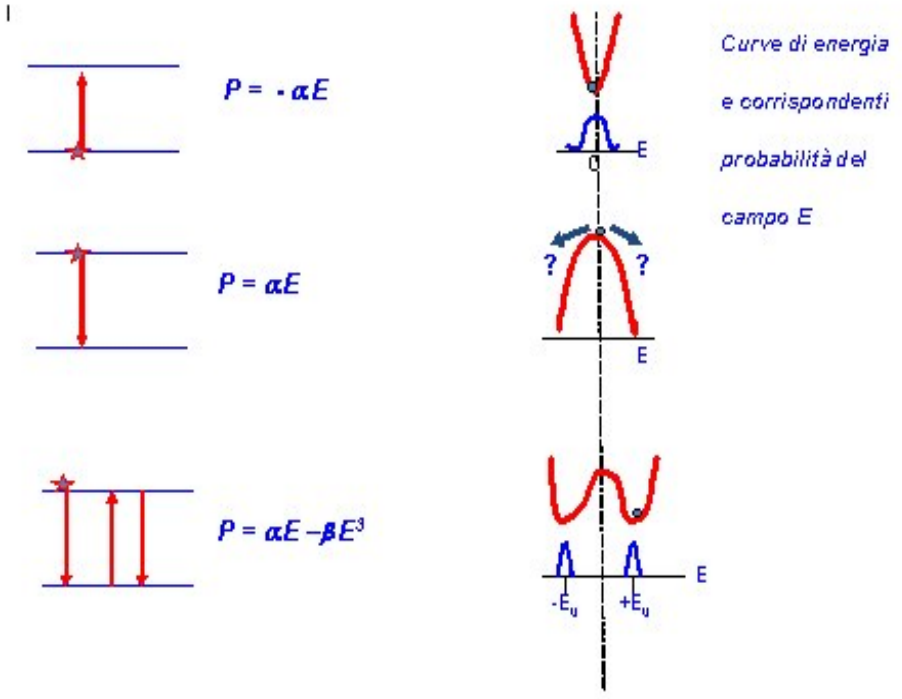

Fig.6 A two-level atom resonantly coupled to an optical field *E*. If the atom is in the ground state (upper part) it absorbs light and contributes a polarization *P* negative in the field. The interaction energy $-P \bullet E$ is a convex parabola (upper right) and the corresponding equilibrium probability for the field has a maximum at the minimum of the parabola; in fact it is a Gaussian as expected for a blackbody field .
As the atom is excited to the upper state(medium part) ,it will emit a photon and the polarization changes sign. The corresponding parabola is concave and there is no minimum where to confine the field, which then should escape (left or right) toward high *E* values; no finite area probability can be defined.
However ,as *E* achieves high values, there is a finite probability that the atom reabsorbs a photon going again to the excited state and then re-emits a photon(lower part). The overall process, implying 3 photons, is less efficient than an independent photon emission from 3 excited atoms; thus it amounts to a negative correction of the polarization cubic in *E*. The corresponding energy is quartic in *E*; it has 2 minima symmetric around the origin. The field probability has 2 peaks at those minima. If the peaks are narrow, they can be assimilated to delta-like distributions at $+Eo$ and $-Eo$, yielding a unique Poisson *PS* around $<n>=|Eo|^2$

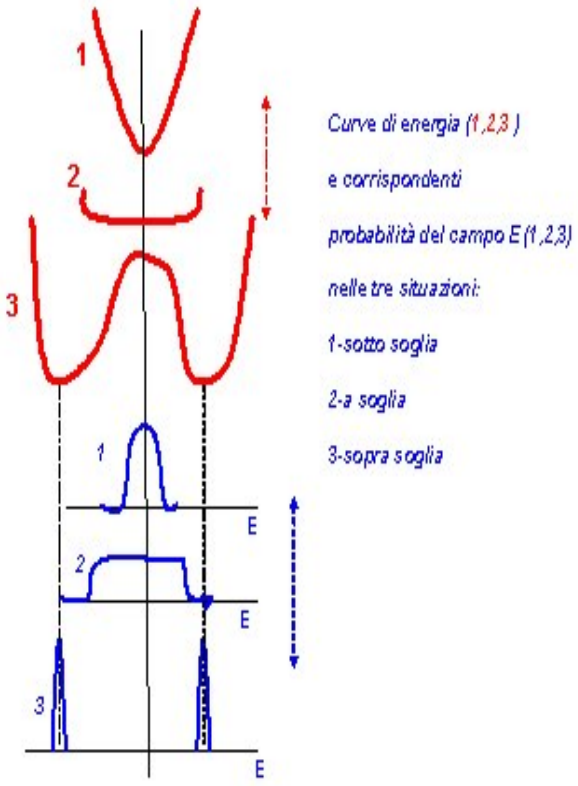

Fig.7 Varying the laser gain-to-loss ratio, a threshold is crossed where the stimulated emission gain compensates the losses. Case 1 is below threshold with a confining parabola and a corresponding Gaussian field probability; case 3 is well above threshold with two narrow peaks of field probability. In between, case 2 (threshold: gain=losses) has zero linear polarization and hence a flat energy bottom ,yielding a broad probability distribution .

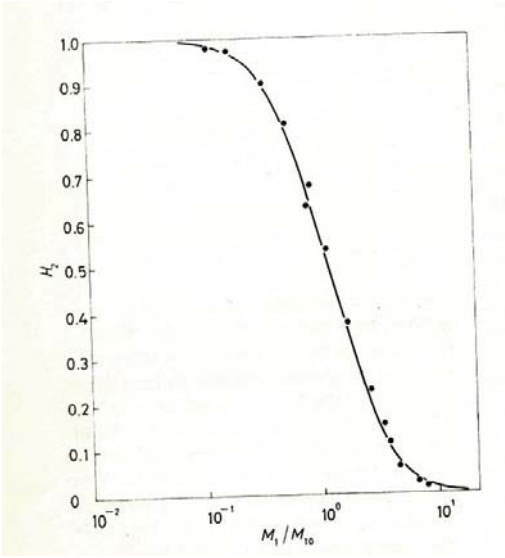

Momento secondo H_2 attorno alla soglia M_1=M_{10} (Arecchi et al 1966)

Fig8-H_2 is the second moment of a laser *PS*, suitably scaled so that it is 1 for a Gaussian field and 0 for a coherent one, versus the ratio between M_1 (first order moment of *PS*, that is, laser intensity) and its threshold value M_{10} .Points are experimental; solid line from Haken's theory[A.33]

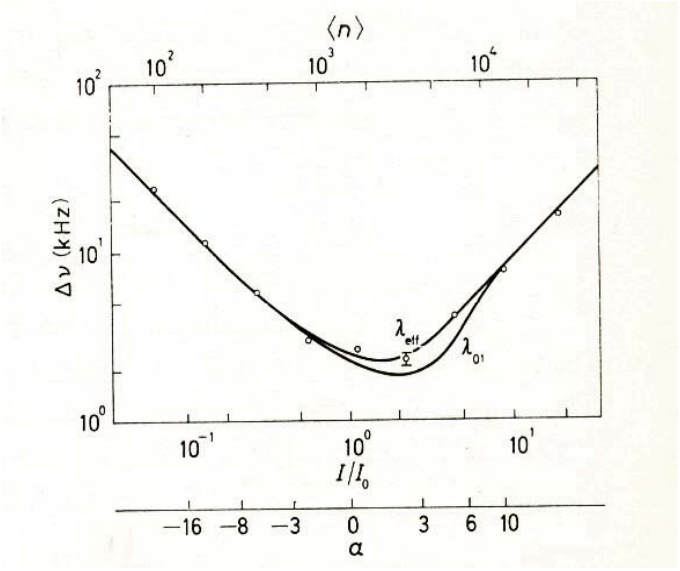

Critical slowing down alla soglia a=0 , <n>=1700 (Arecchi et al 1966)

Fig9- Linewidth of the laser fluctuations versus the intensity ratio to threshold *I/Io*. The experimental points fit the full solution λ_{eff} , whereas the linear approximation linewidth λ_{01} is wrong around threshold. The horizontal axis is also graded by the so called pump parameter a; it is the difference gain – losses; a=0 is the threshold.The upper horizontal axis is the average intra-cavity photon number for each a; for a=0,it is about 1700 for the used laser.[A.36]

Statistiche fotoni (intervallo osservazione 50 nsec) per vari ritardi dal switch (Arecchi et al 1967)

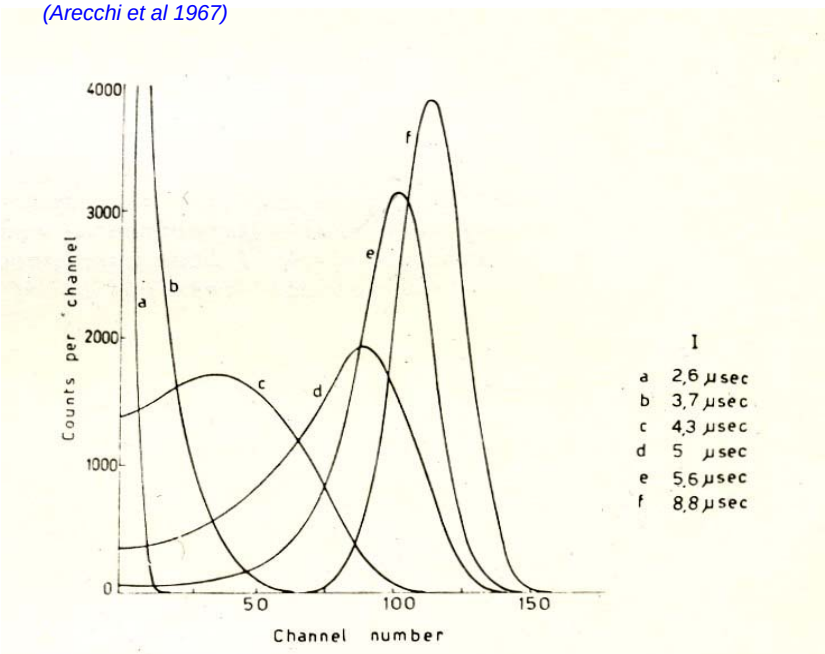

Fig 10-Transient laser PS .As a fast intra-cavity shutter is switched from closed to open, the losses switch from a high to a low value. The transient in a He-Ne laser takes about 10 microsec. If we probe the *PS* over short observation times (50 nsec) at different delays from the switch time we obtain different *PS* (normalized to equal area) ranging from the black-body statistics at the beginning (a)to a Poisson statistics at the end (f) . In order to collect the ensemble of experimental points of each *PS*, once a delay has been set and a single sample collected, the shutter is switched off and the measurement cycle repeated for that same delay.[A.32,35]

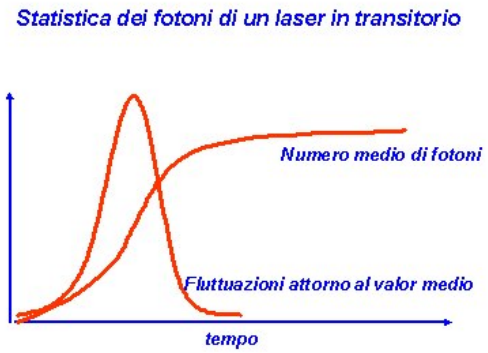

Fig 11.Transient laser statistics: the average photon number has a monotonic increase, whereas the variance undergoes a large intermediate peak. The explanation is that the initial field fluctuations are initially linearly amplified, before being limited by the cubic gain saturation.[A.32]

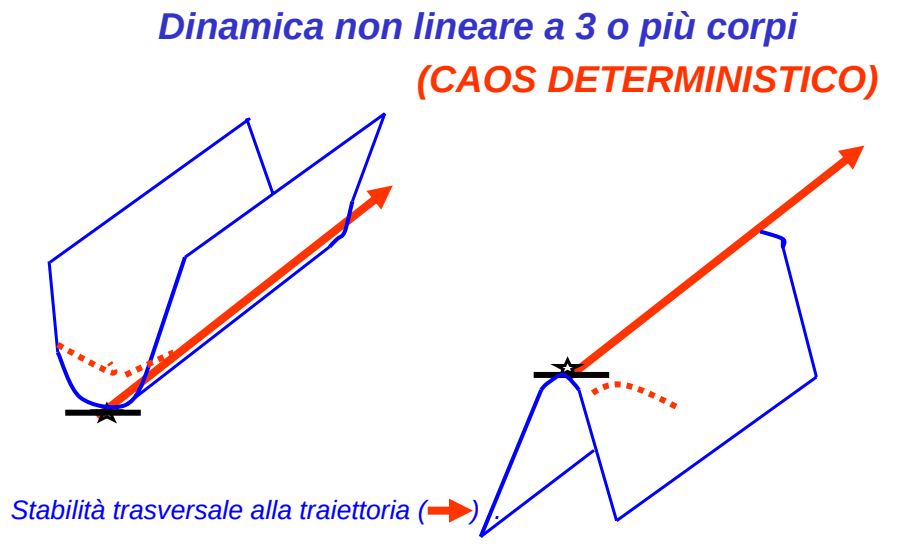

Fig12 *Deterministic chaos*-the trajectory emerging from a precise initial condition ,as the star, is unique. However, in general the initial condition is spread over a small patch. Points of the patch converge toward the calculated trajectory or diverge from it, depending on whether the transverse stability stability landscape is a valley (left) or a hill (right). From 3 coupled dynamical degrees of freedom on, the right situation is generic. we call it *deterministic chaos* . The information loss rate K is called Kolmogorov entropy

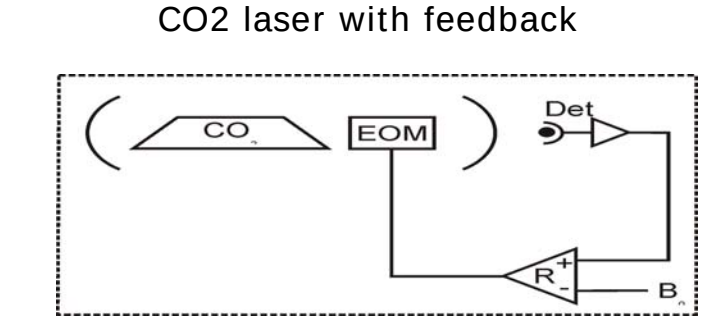

Skeleton of the 3D model

$$\dot{x} = -k_0 x(1 - k_1 \sin^2 z) + Gxy,$$
$$\dot{y} = -2Gxy - \gamma y + p_0,$$
$$\dot{z} = \beta(-z + b_0 - R \cdot x).$$

X laser intensity
Y population inversion
z feedback signal (1986)

Fig13 –*CO2* laser with feedback: experimental set up and the 3 coupled equations. *CO2* is the gas where an electric discharge provides molecular population inversion at the laser frequency; *EOM* is an electro-optic loss modulator driven by the voltage z of the feedback loop; *R* is the gain of the feedback amplifier and *Bo* a d.c. bias voltage [A.134]

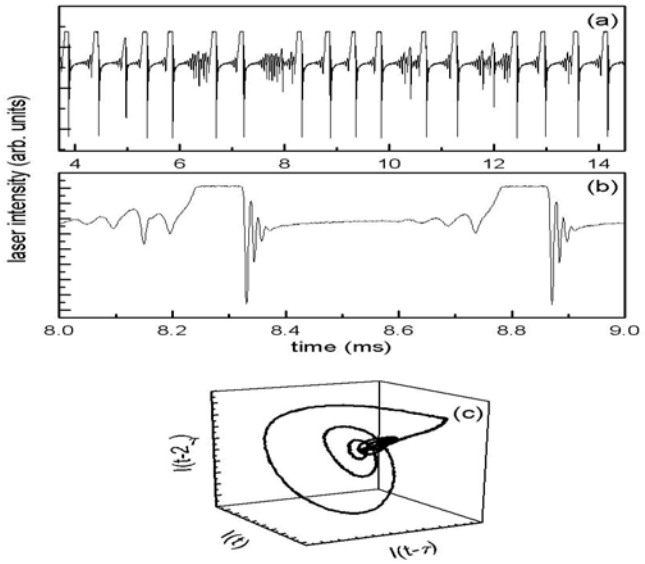

Fig 14-a) trains of almost equal intensity spikes, separated by erratic inter-spike intervals (ISI). b) zoom on two successive spikes, to show their repeatability. c) 3-D phase space built by an embedding technique. Each point reports the intensity sampled at time t and after two short delays τ and 2τ. The figure is built over many spikes. The part of the orbit with a single line is the superposition of the large spikes, the small chaotic tangle corresponds to the small non-repetitive pulses.[A.286]

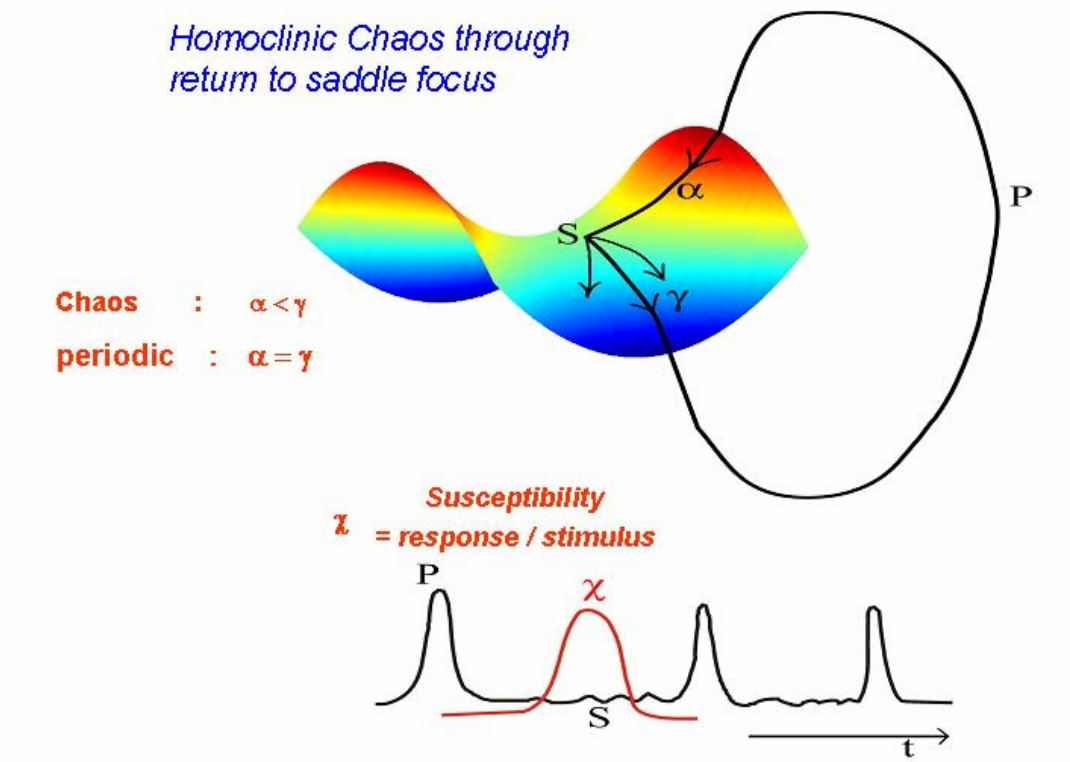

Fig15- *HC (homoclinic chaos*) consisting of the return to saddle focus *S*. The trajectory approaches *S* through a stable branch, and escapes away through an unstable one. We call α the contraction rate and $\gamma \pm i\omega$ the complex expansion rate. If $\alpha < \gamma$,(Shilnikov condition),we have chaos . At *S* the system has a high susceptibility $\chi = response / stimulus$. Away from *S*, the system is insensitive to external perturbations and displays a repeatable loop. Time-wise, large spikes *P* of equal shape repeat at chaotic inter-spike intervals *(ISI).*

(2001)

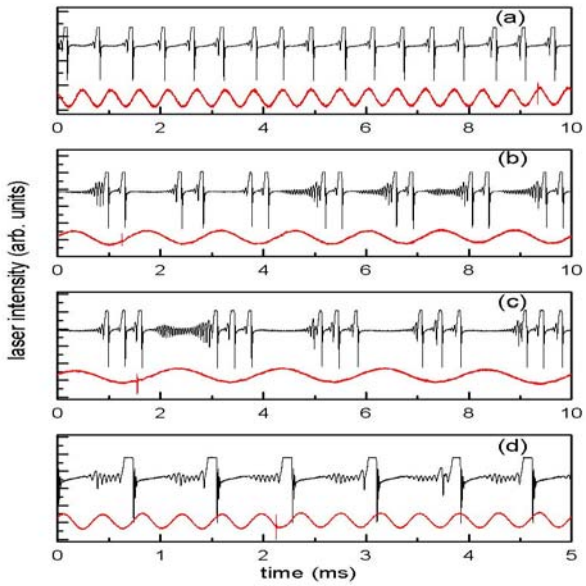

Fig.16- Laser synchronization to a small forcing signal of frequency close to (a) or smaller (b and c)or larger (d) than, the natural HC frequency $2\pi / < ISI >$.[A.286]

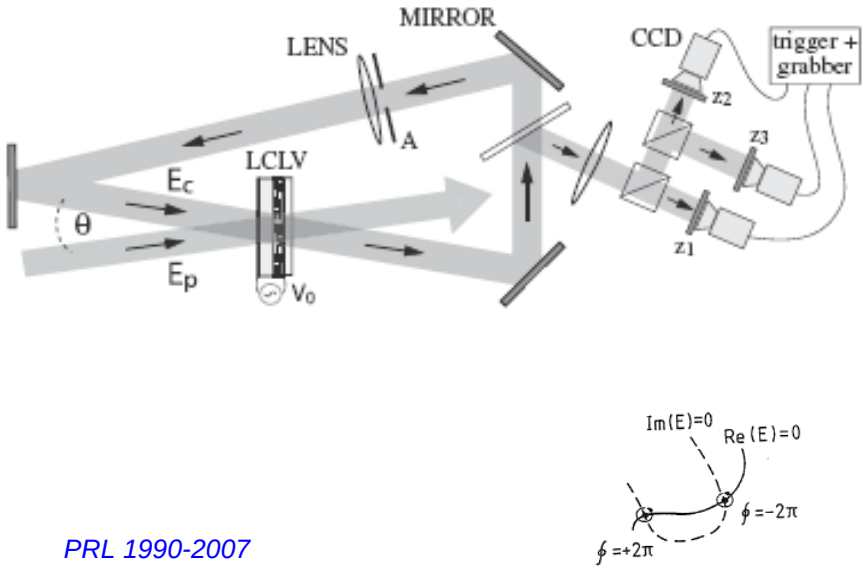

PRL 1990-2007

Fig 17 - Photorefractive oscillator, with the photorefractive effect enhanced by a LCLV(Liquid Crystal Light Valve)- Experimental setup; *A* is an aperture fixing the Fresnel number of the cavity, z =0 corresponds to the plane of the LCLV; z_1, z_2, z_3 are the three different observation planes. Below: 2-dimensional complex field, with lines of zero real part (solid) and lines of zero imaginary part (dashed).At the intersection points the field amplitude is zero and its phase not defined , so that the circulation of the phase gradient around these points is non-zero (either $\pm 2\pi$) yielding phase singularities.[A.177,202,341]

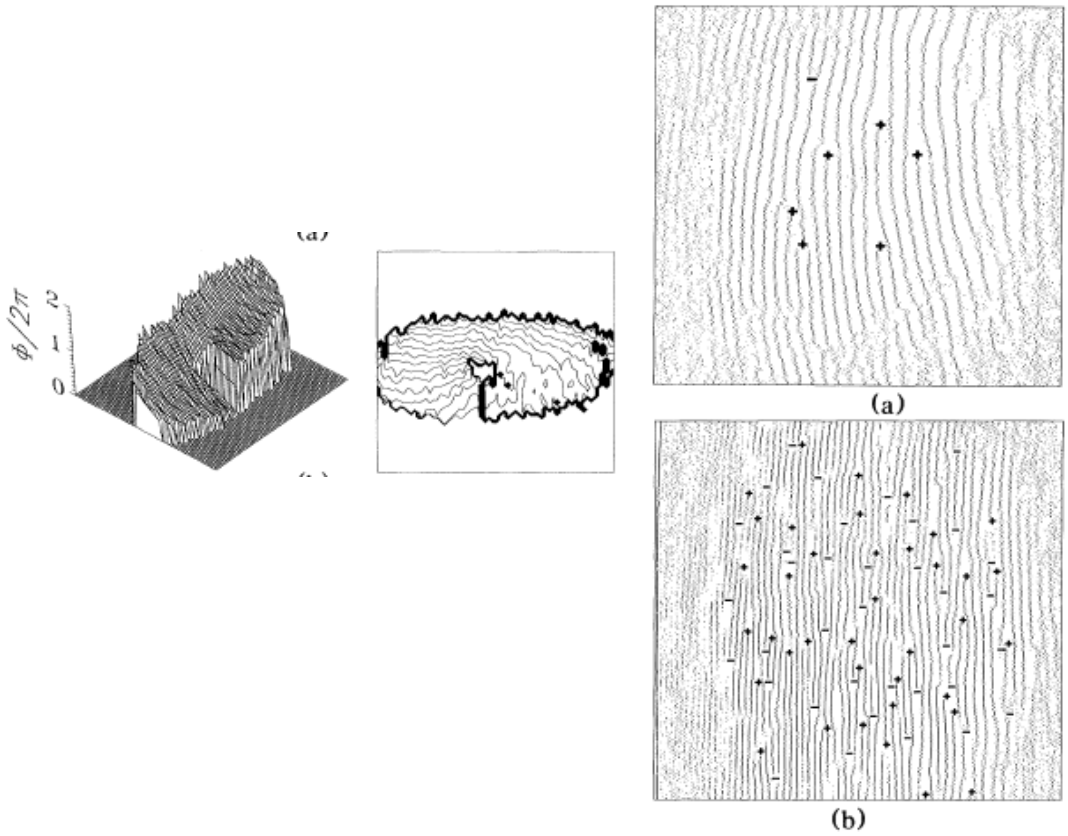

Fig 18 Left : a phase singularity is visualized by superposing an auxiliary coaxial plane wave to the optical pattern of the photorefractive oscillator ;reconstruction of the instantaneous phase surface: perspective and equi-phase plots .

Right: if the auxiliary beam is tilted, we obtain interference fringes, interrupted at each phase singularity ($\pm$ correspond to $\pm 2\pi$ circulation, respectively). The digitized fringe plots correspond to : upper plot (Fresnel number about 3):6 defects of equal topological charge against 1 of opposite charge; lower plot (Fresnel number close to 10) : almost 100 singularities with balanced opposite charges ,besides a small residual unbalance [A.183]

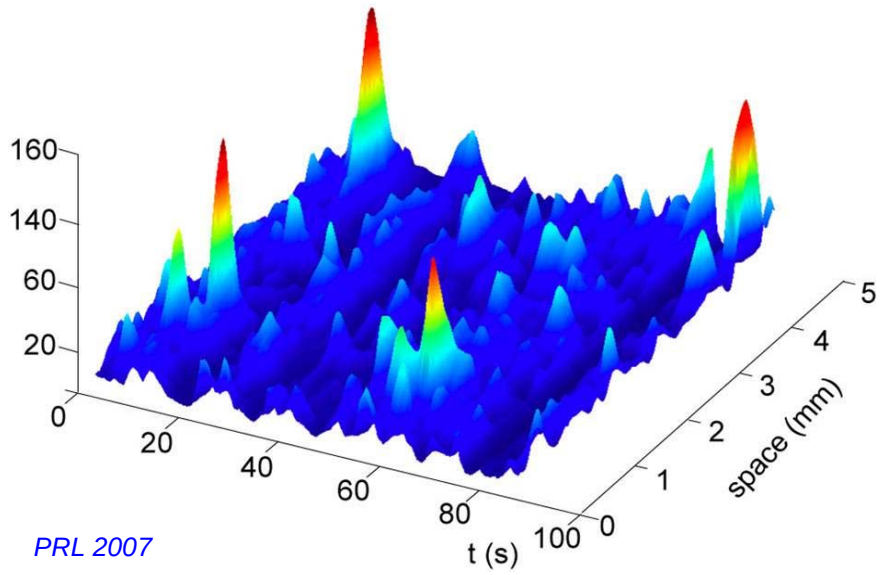

Fig 19 Photorefractive oscillator: Spatiotemporal profile extracted from the z_2 movie.[A.341]

Feature binding (legame di configurazione)

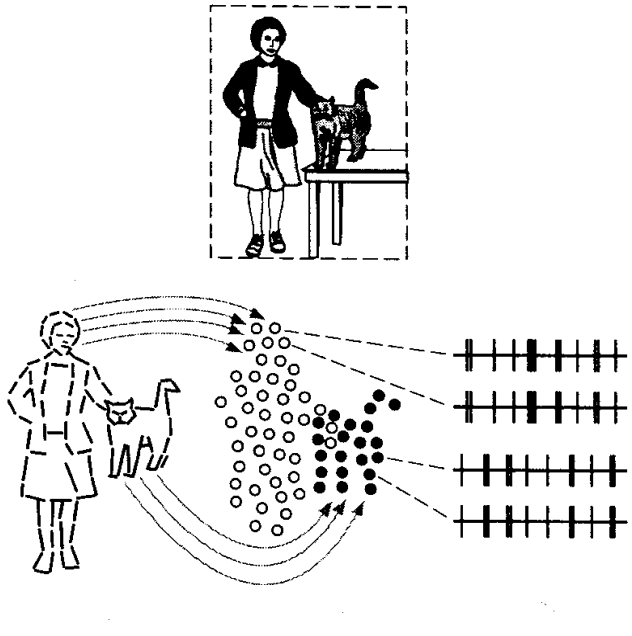

Ogni cerchietto rappresenta un campo ricettivo che isola dettagli specifici (ad es. barra verticale).

Fig.20 **:** Feature binding: the lady and the cat are respectively represented by the mosaic of empty and filled circles, each one representing the receptive field of a neuron group in the visual cortex. Within each circle the processing refers to a specific detail (e.g. contour orientation). The relations between details are coded by the temporal correlation among neurons, as shown by the same sequences of electrical pulses for two filled circles or two empty circles. Neurons referring to the same individual (e.g. the cat) have synchronous discharges, whereas their spikes are uncorrelated with those referring to another individual (the lady) [Singer].

ART = Adaptive Resonance Theory

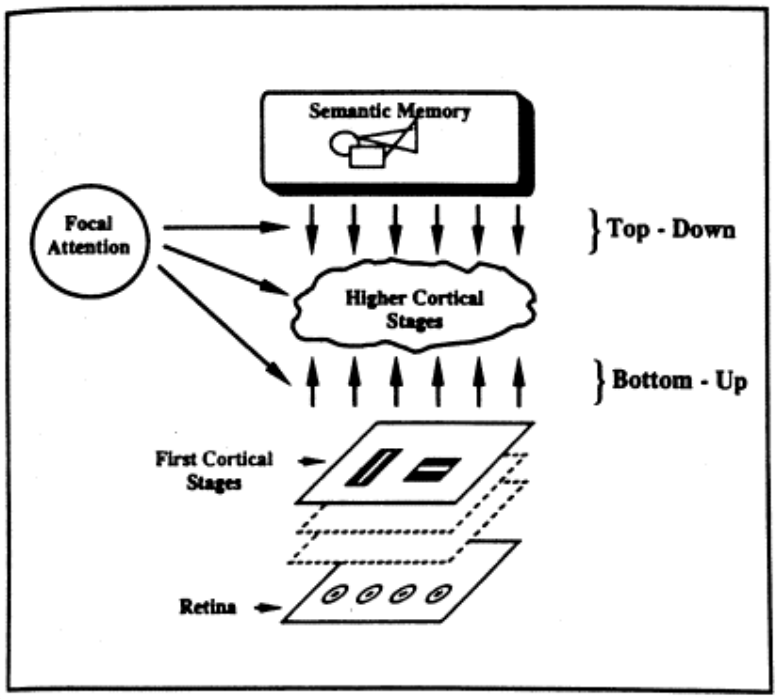

S.Grossberg

Fig. 21: ART = *Adaptive Resonance Theory*. Role of *bottom-up* stimuli from the early visual stages an *top-down* signals due to expectations formulated by the semantic memory. The focal attention assures the matching (resonance) between the two streams.[Grossberg]

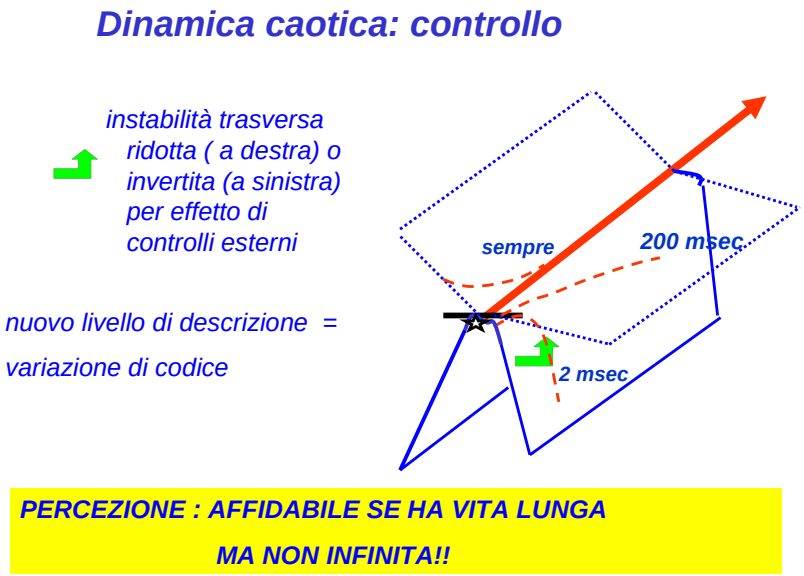

Fig.22-- Chaos is controlled by adding extra-dynamic variables, which change the transverse instability without affecting the longitudinal trajectory. In the perceptual case, the most suitable top-down signals are those which provide a synchronized neuron array with an information lifetime sufficient to activate successive decisional areas (e.g. 200 ms), whereas the single HC neuron has a chaotic lifetime of 2 ms. If our attentional-emotional system is excessively cautious, it provides a top-down correction which may stabilize the transverse instability for ever, but then the perceptual area is blocked to further perceptions.

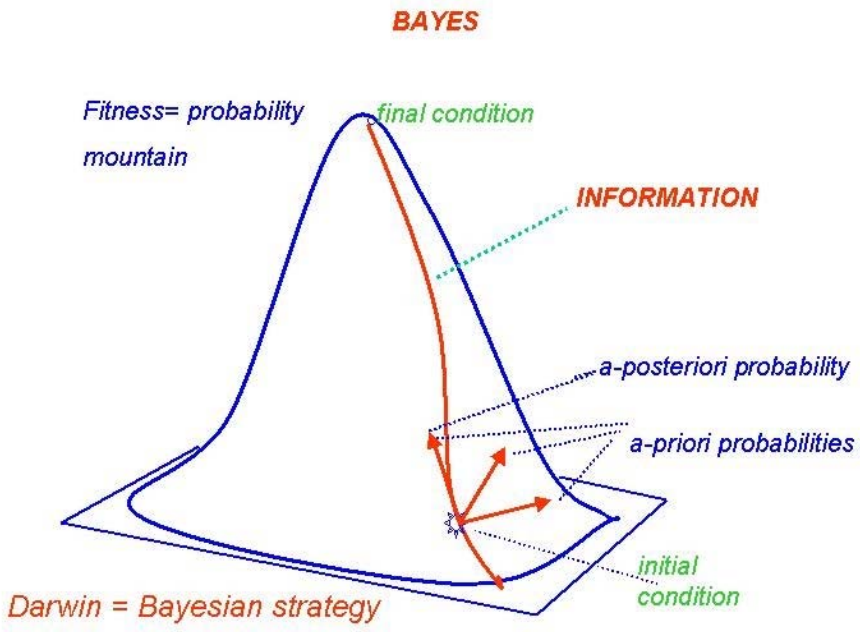

Fig. 23-. Successive applications of the Bayes theorem to the experiments. The procedure is an ascent of the Probability Mountain through a steepest gradient line. Each point of the line carries an information related to the local probability by Shannon formula. Notice that Darwinian evolution by mutation and successive selection of the best fit mutant is a sequential implementation of Bayes theorem.[A.349,352]

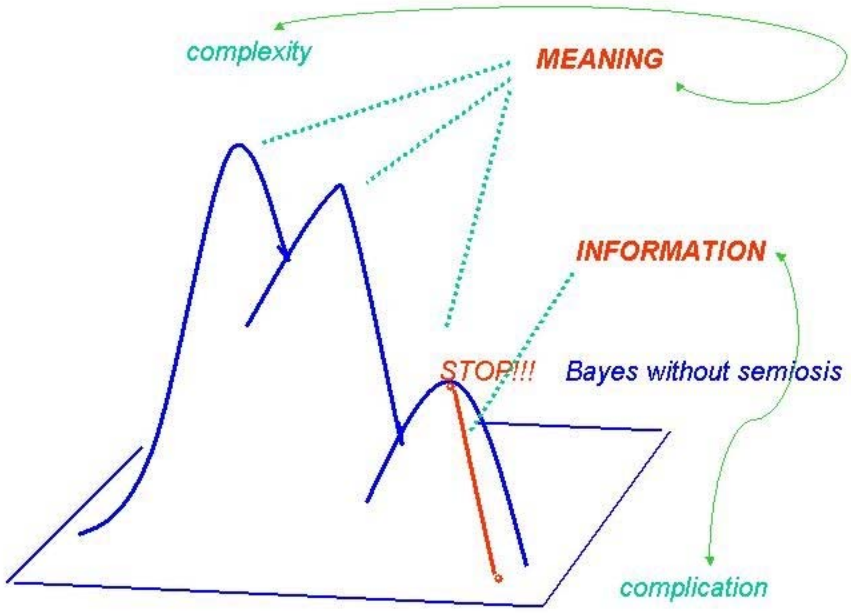

.

Fig.24-Semantic complexity – A complex system is one with a many-peak probability landscape. The ascent to a single peak can be automatized by a steepest gradient program. On the contrary, to record the other peaks, and thus continue the Bayes strategy elsewhere, is a creativity act, implying a holistic comprehension of the surrounding world (*semiosis*). We call "*meaning*" the multi-peak landscape and "*semantic complexity*" the number of peaks. It has been guessed that semiosis is the property that discriminates living beings from Turing machines [Sebeok]; here we show that a non-algorithmic procedure, that is, a non-Bayesian jump from one model to another is what we have called creativity. Is semiosis equivalent to creativity? [A.349,352]

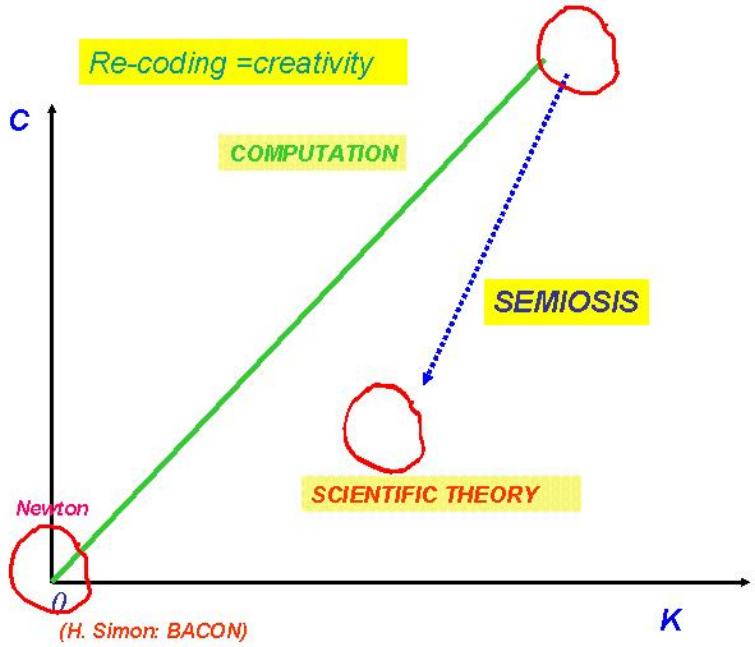

Fig.25- C-K diagram (C=computational complexity; K=information loss rate in chaotic motion): Comparison between the procedure of a computer and a semiotic cognitive agent (say: a scientist). The computer operates within a single code and C increases with K. A scientist explores how adding different degrees of freedom one can reduce the high K of the single-code description. This is equivalent to the control operation of Fig.22; it corresponds to a new model with reduced C and K. An example is offered by the transition from a molecular dynamics to a thermodynamic description of a many body system. Other examples are listed in Table 1.The BACON program [Simon]could retrieve automatically Kepler's laws from astronomical data just because the solar system approximated by Newton two-body interactions is chaos-free.